Supporting Information

The solvent and zinc source dual-induced synthesis of a two dimensional zeolitic imidazolate framework with farfalle-shape and its crystal transformation to zeolitic imidazolate framework-8

Chun-Xin Jin, [b] Yu Wang, [c] Qiu-Shan Gao, [b] Dan-Yang Yao, [d] Si-Hong Wang, [a] Donghao Li,*[a, b] and Hai-Bo Shang*[a, b]

[a] Key Laboratory of Biological Resources of the Changbai Mountain & Functional Molecules (Yanbian University), Ministry of Education, Park Road 977, Yanji City, Jilin Province, 133002, China

[b] Department of Chemistry, Yanbian University, Park Road 977, Yanji City, Jilin Province, 133002, China

[c] State Key Laboratory of Separation Membranes and Membrane Processes, School of Material Science and Engineering, Tianjin Polytechnic University, Tianjin, 300387, China

[d] Agricultural college of Yanbian University, Park Road 977, Yanji City, Jilin Province, 133002, China

E-mail: dhli@ybu.edu.cn; hbshang@ybu.edu.cn

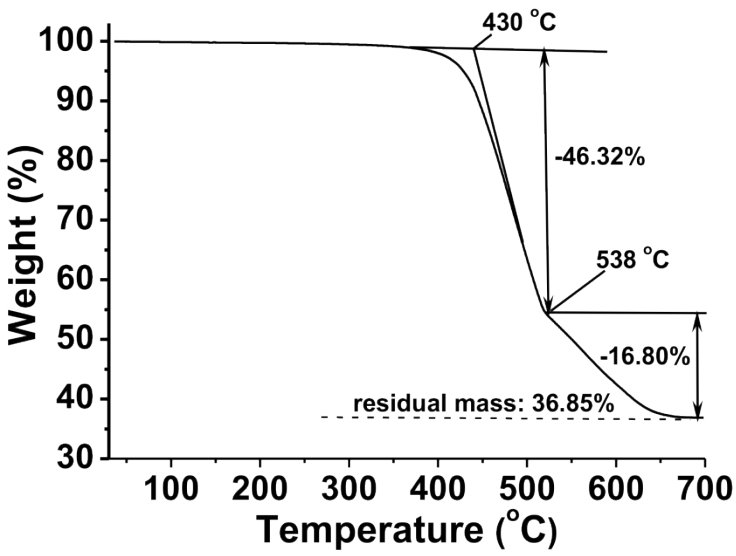

Fig. S1 TG analysis of ZIF-F after activation at 120 °C for 12 h.

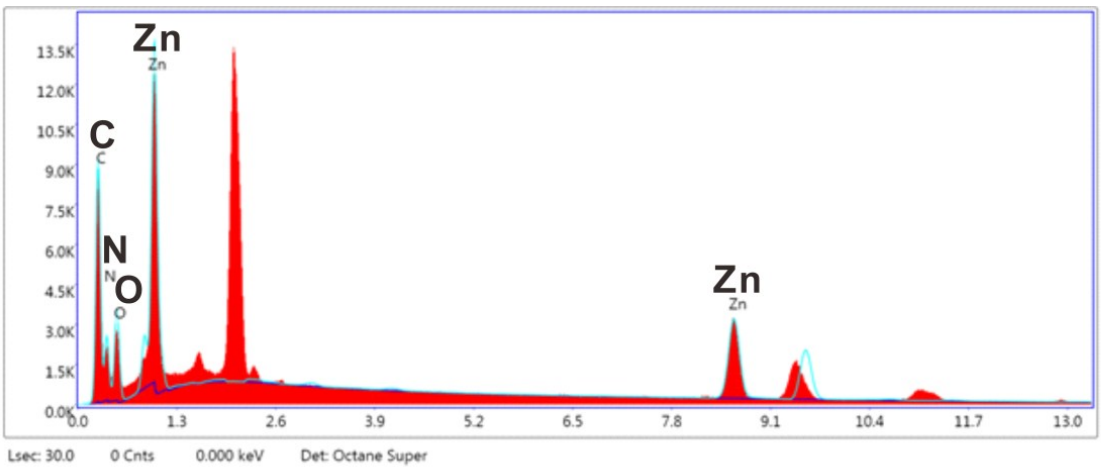

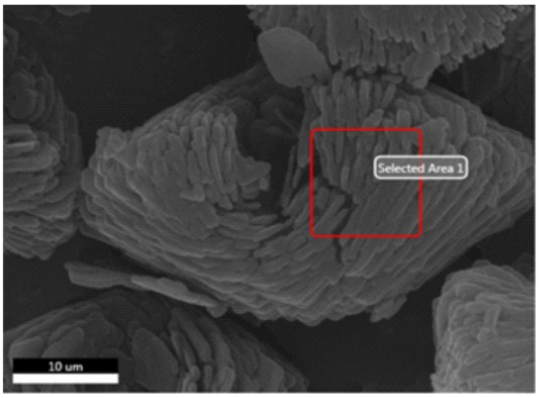

Element	Weight %	Atomic %
C	35.19	48.38
N	23.60	27.83
O	17.15	17.71
Zn	24.06	6.08
Total	100.00	100.00

Fig. S2 EDX analysis of ZIF-F.

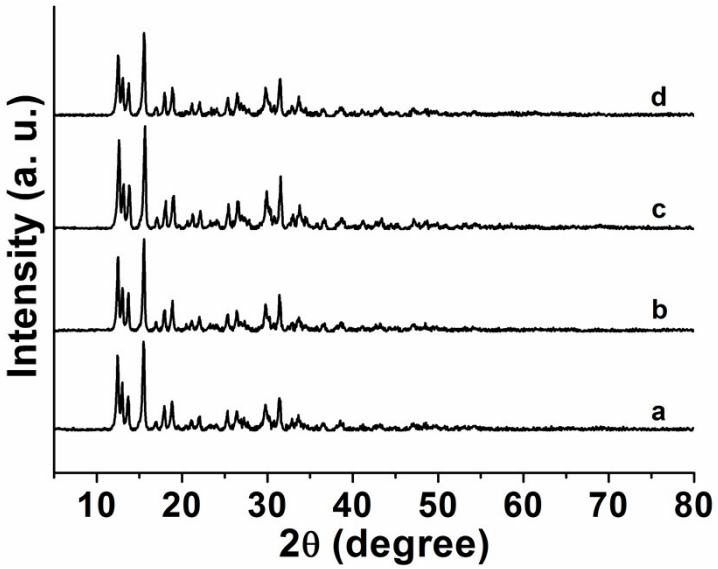

Fig. S3 XRD patterns of re-produced ZIF-F samples: (a, b, c) three repetitions with the normal system, (d) A fivefold expansion of the synthesis system.

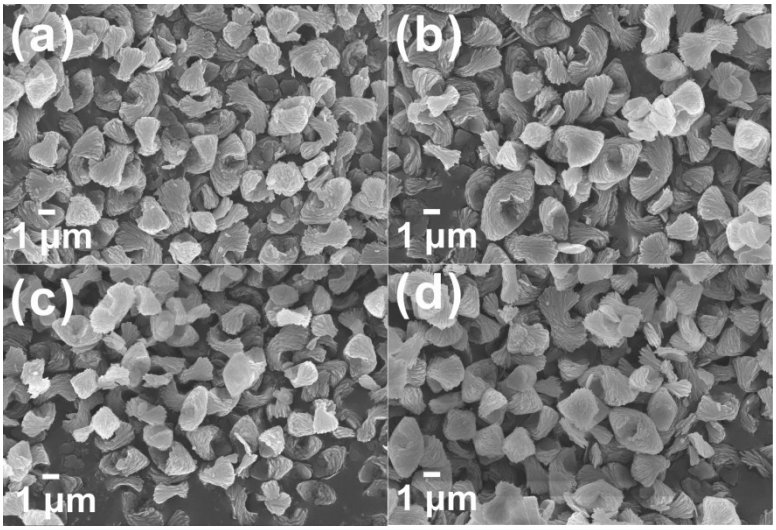

Fig. S4 SEM images of re-produced ZIF-F samples: (a, b, c) three repetitions with the normal system, (d) A fivefold expansion of the synthesis system.

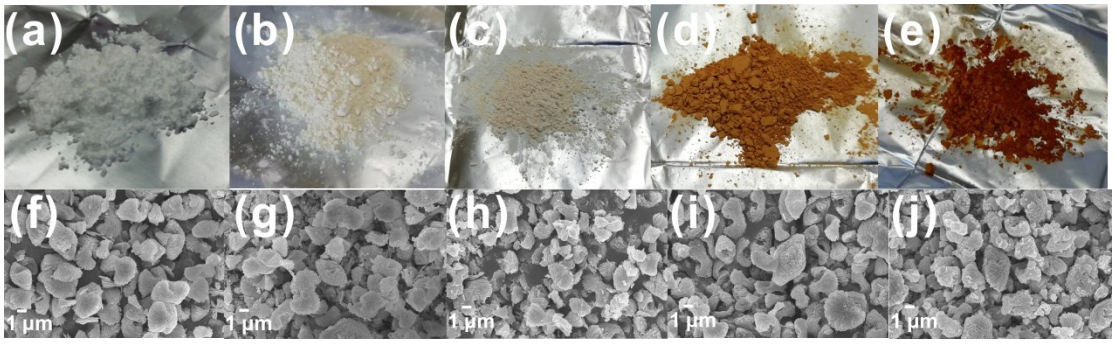

Fig. S5 Photo pictures and SEM images of ZIF-F before and after thermal treatments under different temperatures for 12 h: (a, f) before heating, (b, g) 200 ^{o}C, (c, h) 300 ^{o}C,

(d, i) 350 °C, (e, j) 400 °C.

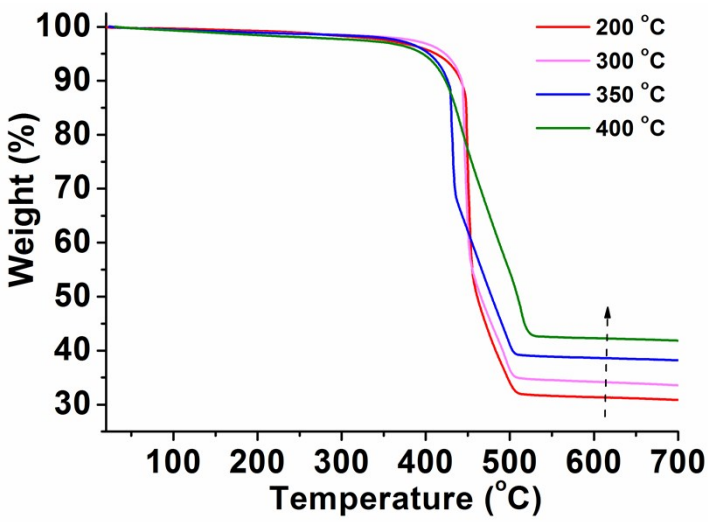

Fig. S6 TG analysis of the calcined samples after 200, 300, 350, 400 °C for 12 h , respectively.

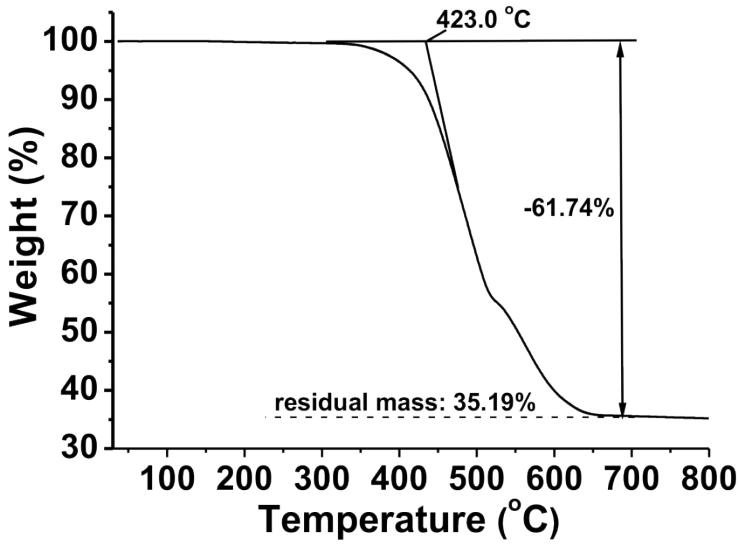

Fig. S7 TG analysis of the prepared ZIF-8.

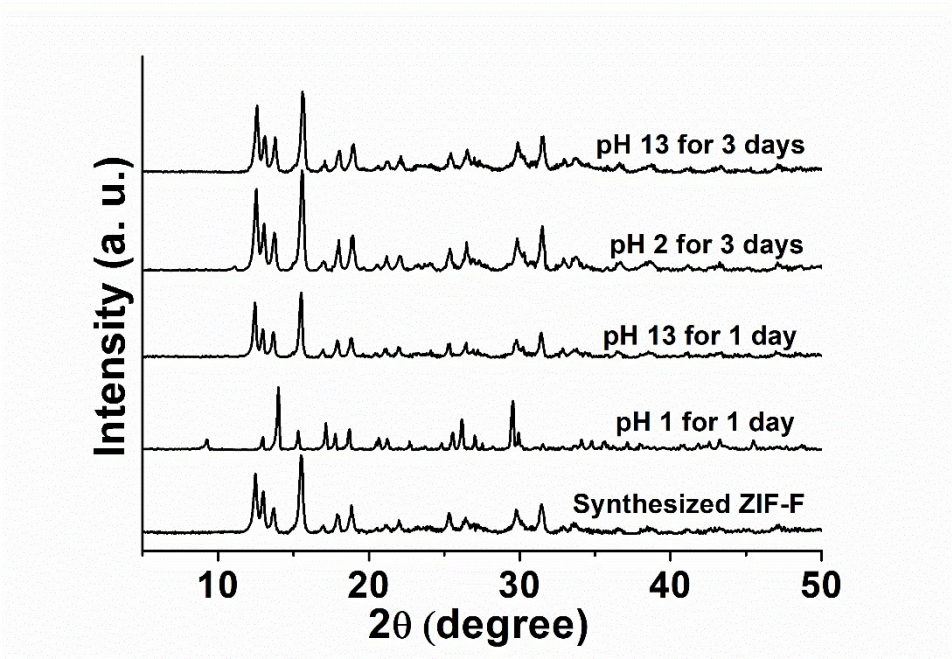

Fig. S8 XRD patterns of ZIF-F after immersion in acid and basic solutions.

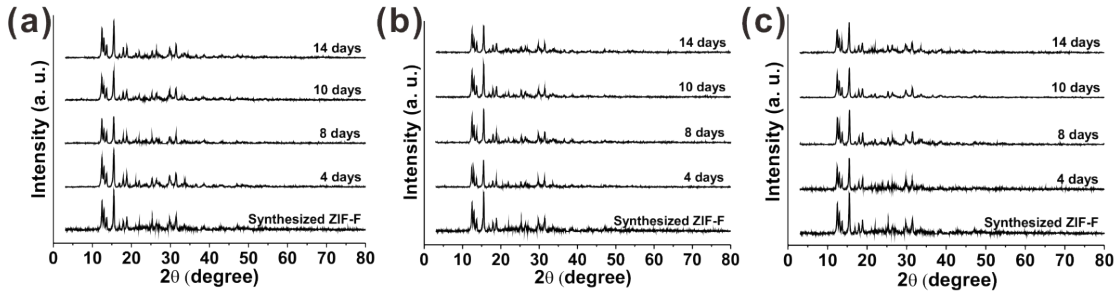

Fig. S9 XRD patterns of ZIF-F after immersion in organic solvents: (a) DMF, (b) DCM, (c) toluene.

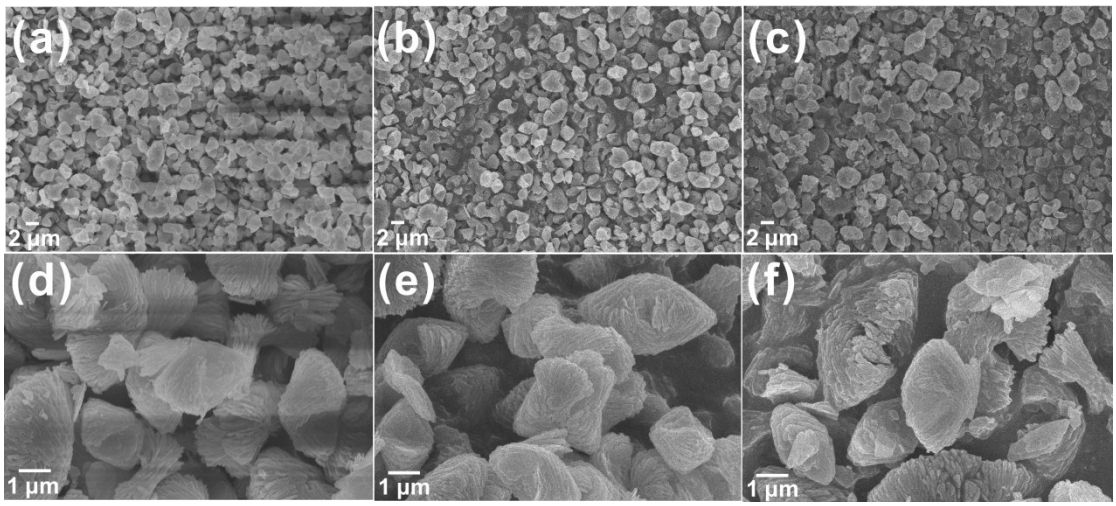

Fig. S10 SEM images of ZIF-F after immersion in organic solvents for 14 days: (a, d) DMF, (b, e) DCM, (c, f) toluene.

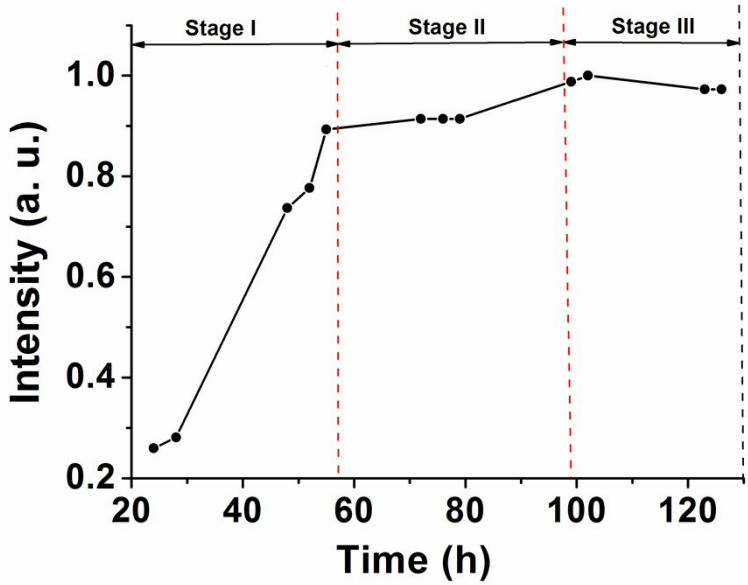

Fig. S11 Curve of extent of crystallization (α) as a function of time (t) obtained from time-resolved in situ ^{1}H NMR.

Avrami's Analysis

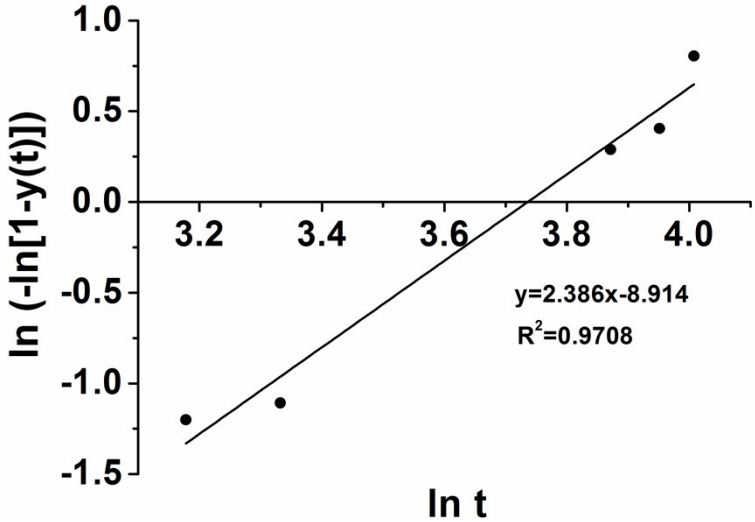

Fig. S12 The linear regression analysis of Avrami's classical model.

Avrami's Equation

$$1 - y(t) = e^{kt^n} \quad \text{(S1)}$$

Linear form of Avrami's Equation

$$\ln(-\ln[1 - y(t)]) = lnk + nlnt \quad \text{(S2)}$$

Where *t* is the synthesis time, *k* is the scaling constant, *n* is Avrami's constant and y(*t*) is the ZIF-8 relative crydtallinity as a function of time.

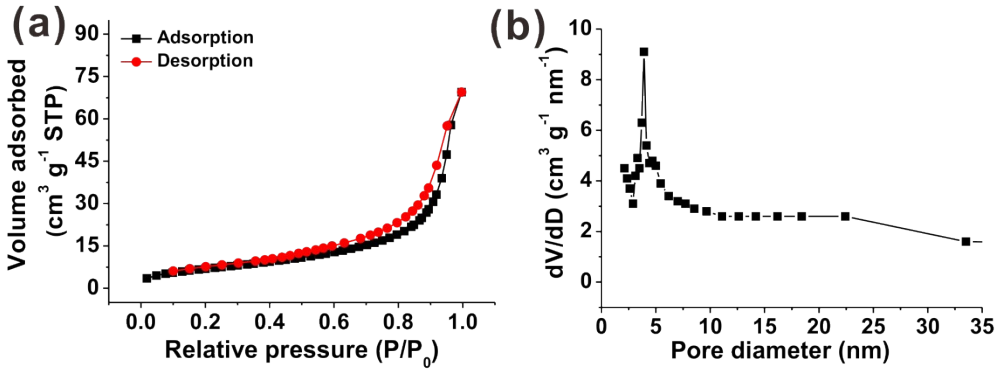

Fig. S13 (a) Nitrogen adsorption-desorption isotherm of ZIF-F at 77.3 K, (b) Pore diameter distribution of ZIF-F obtained by BJH method.

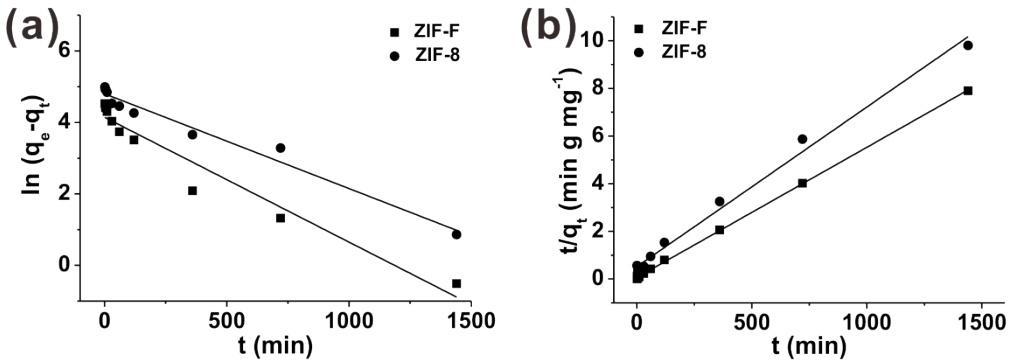

Fig. S14 The pseudo-first-order kinetic models (a) and pseudo-second-order kinetic models (b) of ZIF-F and ZIF-8.

Table S1 Kinetic parameters of ZIF-F and ZIF-8 for the CR adsorption

	pseudo-second-order kinetic model			pseudo-first-order kinetic model	
	$q_{e(cal)}$ (mg g^{-1})	k_2 (g mg^{-1} min^{-1})	R^2	k_1 (min^{-1})	R^2
ZIF-F	182.82	4.93×10^{-4}	0.9996	3.49×10^{-3}	0.9425
ZIF-8	149.25	8.69×10^{-5}	0.9908	2.65×10^{-3}	0.9687